21 Neutron Stars

If a stellar remnant exceeds the Chandrasekhar mass, then even fully relativistic electron degeneracy pressure will be insufficient to support it. As we discussed in Sec. 19.4, only neutron degeneracy pressure can possible halt its final and inevitable collapse. Let's now consider the astrophysics of neutron stars in more detail.

21.1 *Neutronic Chemistry*

For starters: why don't all the neutrons just decay away? An isolated neutron undergoes the decay

(528) $n \to p + e^- + \bar{\nu}_e$

because

(529) $(m_n - m_p)c^2 = 1.3 \text{ MeV}.$

The excess energy will be carried away by the electron and antineutrino.

But in a degenerate medium, the Fermi energy may exceed this 1.3 MeV limit. When this happens, there are no accessible low-energy states for the electron to occupy after decay – so the neutron decay is suppressed (alternatively, imagine the neutron decays but it is energetically favorable for the new electron to immediately recombine with an available proton). We expect this beta-decay suppression to set in when

(530)
$$E_F \gtrsim (m_n - m_p)c^2 = 1.3 \text{ MeV}$$

(531)
$$\sqrt{p_F^2 c^2 + m_e^2 c^4} \gtrsim (m_n - m_p)c^2$$

(532)
$$m_e c^2 \left(\frac{p_F^2}{m_e^2 c^2} + 1 \right)^{1/2} \gtrsim (m_n - m_p)c^2.$$

So to keep the neutrons around, the Fermi momentum must satisfy

(533) $$p_F \gtrsim m_e c \left[\left(\frac{m_n - m_p}{m_e} \right)^2 - 1 \right]^{1/2}$$

or roughly $p_F c \gtrsim 1.2$ MeV. In terms of density, we refer to Eq. 395,

$$p_F = \left(\frac{3n^3 \rho}{8\pi m_p} \right)^{1/3}.$$

So combining this with Eq. 533 we see that neutron decay is suppressed for

(534) $\rho \gtrsim 10^7$ g cm^{-3}.

As ρ_c reaches and exceeds this critical density, the neutron star establishes an equilibrium between neutrons, protons, and electrons. One can develop a Saha-like equation (recall Sec. 8.5) relating the populations of each type of particle; see Sec. 2.6 of Shapiro & Teukolsky for further details. Above the critical density, the so-called **neutron drip** sets in and neutrons slowly leave the individual nuclei. In the extreme end case, the star is indeed entirely neutrons.

21.2 *Tolman-Oppenheimer-Volkoff*

Note also that for neutron stars,

(535) $$\frac{GM}{rc^2} \approx 0.1 - 0.3$$

and so we are definitely in a range where Newtonian gravity alone will not suffice. General relativity must be used instead.

Recall from Sec. 5 that gravity determines the geometry of spacetime, so that the interval (or distance) ds between two events is

(536) $$ds^2 = g_{\mu\nu} dx^\mu dx^\nu$$

where $g_{\mu\nu}$ is the metric and dx^μ is the coordinate displacement between two events (see Eqs. 12 and 14).

For a spherical, static body, general relativity shows that the appropriate metric is

(537) $$ds^2 = -e^{2\Phi(r)/c^2}(cdt)^2 + \frac{dr^2}{1 = 2GM/rc^2} + r^2(d\theta^2 + \sin^2\theta d\phi^2)$$

where as usual

(538) $$M(r) = \int_0^r = 4\pi(r')^2 \rho(r') dr'$$

and

(539) $$\frac{d\Phi}{dr} = -\frac{G[M(r) + r\pi r^2 P(r)/c^2]}{r(r - 2GM(r)/c^2)}.$$

The boundary conditions are that

(540) $$e^{2\Phi/c^2} = 1 - \frac{2GM}{rc^2} \quad (r > R_*)$$

(541) $$\rho(r) = 0 \quad (r \geq R_*)$$

These equations build in the relativity of distance and time, plus the fact that all forms of energy (including pressure) contribute to gravity. Ultimately the new, relativistic equation of hydrostatic equilibrium is

$$\frac{dP}{dr} = -\left(\frac{G}{r^2}\right)\left[\frac{M + 4\pi r^3 P/c^2}{1 - 2GM(r)/rc^2}\right]\left[\rho + P/c^2\right]. \tag{542}$$

This is the **Tolman-Oppenheimer-Volkoff equation** (or TOV). Note that in the limit of low densities and pressures, all terms with $1/c^2$ drop out and we recover Eq. 192,

$$\frac{dP}{dr} = -\left(\frac{G}{r^2}\right) M\rho = -\rho g.$$

21.3 *Neutron star interior models*

To make a neutron star model, we need to solve the TOV equation – but we also need to have an equation of state to work with. The trouble is that neutron stars push us into a regime where the physics is not accurately known! But we can still consider a few limiting cases.

The first of these is to assume that the neutron star equation of state is so stiff that it is incompressible, i.e., $\rho(r) = \rho_0 =$ constant. Then (as Problem Set 8 demonstrates),

$$P(r) = \rho_0 c^2 \left[\frac{(1 - R_S r^2/R_*^3)^{1/2} - (1 - R_S/R_*)^{1/2}}{3(1 - R_S/R_*)^{1/2} - (1 - R_S r^2/R_*^3)^{1/2}}\right] \tag{543}$$

where R_* is the radius of the neutron star and

$$R_S = \frac{2GM}{c^2} \tag{544}$$

is the **Schwarzchild radius**. This incompressible model shows that $P(r = 0) \to \infty$ if R_* is too small (i.e., if the NS is too compact). The denominator of Eq. 543 must be > 0, so we obtain the constraint that

$$R_* > \frac{9}{8} R_S = 2.25 \frac{GM}{c^2}. \tag{545}$$

The implication is that a star more compact than this cannot be supported even by infinite pressure; it will collapse instead.

In reality, no fluid can be truly incompressible, since this would require an infinite (and super-luminal) sound speed. Rhodes & Ruffini (1974) developed as stiff a NS model as possible that was still consistent with relativity. Their result was that neutron stars must have $M < 3.2 M_\odot$.

21.4 *A bit more neutron star structure*

More typically in modern studies, one chooses an equation of state – or at least, builds up $P(\rho)$ based on your favorite knowledge/assumptions about

dense matter. One picks a central density (informed by your previous model, perhaps) and integrates Eq. 542 until $P = 0$ is reached; this is the surface. One tabulates M_* and R_* for different equations of state; Fig. 47 shows the range of possible models.

Inspection of Fig. 47 shows that predicted radii and maximum masses vary by $\sim$50% for neutron stars. Typical models (plotted in black) assume "normal" nuclear matter – just standard neutrons at low densities, but at higher densities condensations of hyperons, kaons, pions, etc. may all become important. Different models make different choices for when various mesons (and other particles) play a role. Until the critical density is reached, these models scale roughly as $R_* \propto M_*^{-1/3}$ (as we saw for white dwarfs in Sec. 20.3) since the stars are still explained decently well by straightforward degeneracy calculations.

Another family of models assumes that (under other assumptions) neutron stars may be composed of so-called strange quark matter. These objects would instead be hypothetical condensates of up, down, and strange quarks that would be more stable than normal matter at the high densities involved. In grossly simplified terms, these models amount to a uniform density fluid – so $R_* \propto M_*^{1/3}$.

There are also several forbidden regions:

- **General Relativity:** If a neutron star is to avoid becoming a black hole, it must always satisfy $R > 2GM/c^2$.
- **Causality:** This is the requirement that the soundspeed c_s must satisfy $dP/d\rho = c_s < c^2$.
- **Rotation:** Neutron stars rotate (like stars and other stellar remnants). To

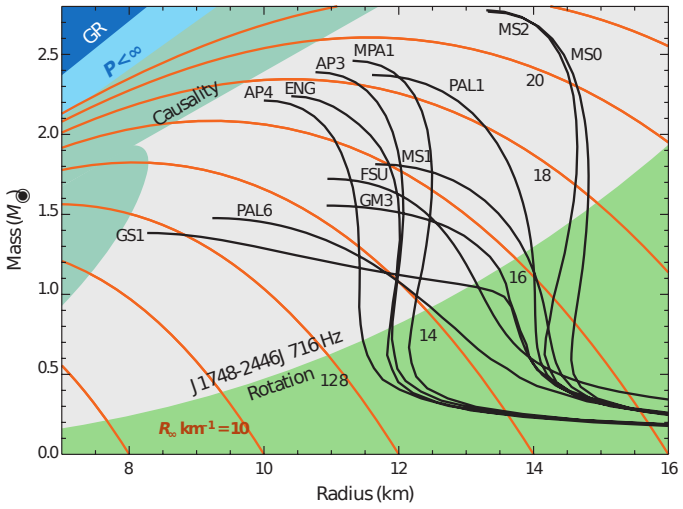

Figure 47: Predicted masses and radii (black curves) for various suggested neutron star equations of state. Orange curves show contours of $R_\infty = R(1 - 2GM/Rc^2)^{-1/2}$. Adapted from Lattimer (2012), *Ann. Rev. Nuc. Part. Sci.*.

hold together, they must satisfy

$$\omega^2 R < \frac{GM}{R^2} \tag{546}$$

or equivalently

$$\omega^2 < \frac{GM}{R^3} \tag{547}$$

and so a spinning neutron star must always satisfy

$$G\rho_{\rm avg} \geq \frac{3\omega^2}{4\pi}. \tag{548}$$

Thus the "rotation" line corresponds to constant average density. In Fig. 47, the particular line plotted corresponds to the fastest-known rotation rate for any neutron star, $f = \omega/2\pi = 716$ Hz.

The orange curves in Fig. 47 indicate lines of constant **radiation radius** R_∞. In principle one could observe the thermal (typically X-ray) spectrum of a young neutron star of known distance, assume a blackbody, and estimate the radius directly. But for such massive, compact objects general relativistic effects will come into play: the temperature, size, and so luminosity observed at large distances are not the "true" values that would be observed in the neutron star's rest frame. In particular, the radiation radius is

$$R_\infty = R_*(1 + z_g) \tag{549}$$

where z_g is the **gravitational redshift** (see Eq. 511). Similarly, the temperature that will be inferred is

$$T_{\rm eff}^\infty = \frac{T_{\rm eff}}{1 + z_g}. \tag{550}$$

21.5 *Neutron Star Observations*

Neutron stars are fairly unique among objects discussed thus far. Planets, stars, nebulae, and galaxies were all observed for millenia before the true natures of these objects were uncovered. In contrast, neutron stars (along with black holes) were discussed theoretically long before any observational evidence was found.

Unfortunately the observational measurements are frustratingly sparse. Even the fastest spin rates don't much push the physical limits. As far as maximum masses go, Fig. 44 shows that most measured NS masses are around $1.4M_\odot$. The few especially massive examples ($M_* \gtrsim 2M_\odot$) do help kill quite a few models, though. And for radii it's worse: while some masses are measured to $\lesssim 2\%$, there are no comparably precise NS radius measurements (despite many efforts). Anyway, only $\sim$10 neutron stars are close enough that we can study their thermal emission (in X-rays; $kT \gtrsim 50$ keV) — if they are more than $\gtrsim 500$ pc away then the ISM absorbs most of the radiation; and even when

detections are made, detailed atmospheric modeling (with many unknowns) is needed to accurately infer radii.

Most observational data of neutron stars come from **pulsars** – neither truly pulsating nor truly stars, but rapidly-rotating neutron stars that emit periodic radio (or other EM) emission. These were first discovered in 1967 by Jocelyn Bell, a 2nd year graduate student.

21.6 *Pulsars*

First discovered in 1967, thousands of pulsars are now known (see Fig. 48). Most are detected in radio, but a subset are also seen in X-rays and even gamma rays. The period of the EM emission ranges from as long as 10 s in a few cases to just 1–2 ms at the other extreme.

It was recognized almost immediately that these objects must be very small. E.g., the Crab nebular pulsar (the remnant of SN 1054) has a period of $P = 33$ msec, implying a maximum diameter of

$$L \lesssim cP = (3 \times 10^5 \text{ km s}^{-1})(0.033) \approx 10^5 \text{ km}. \quad (551)$$

The size is consistent with a white dwarf but the period isn't. From Eq. 547

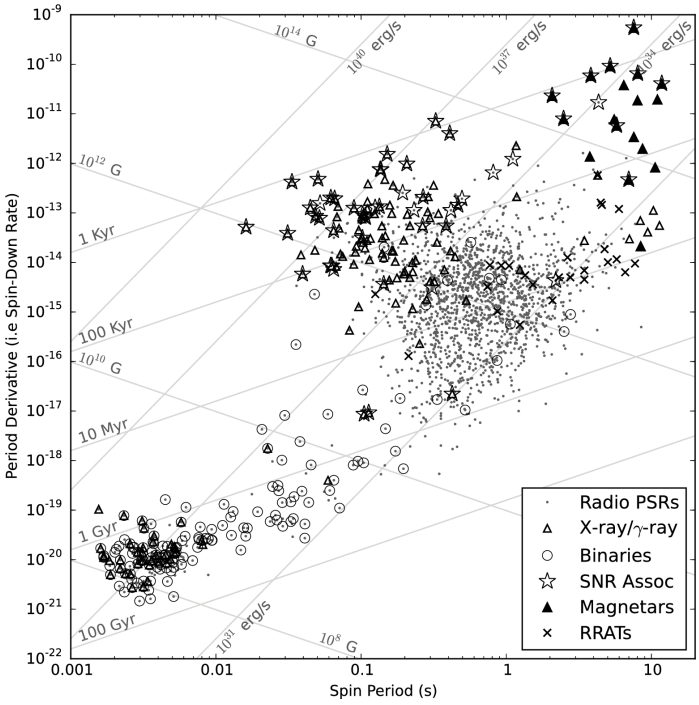

Figure 48: Pulsar observations in the traditional P-$\dot{P}$ plane. Straight lines indicate characteristic ages, spin-down luminosities, and maximum magnetic field strengths. (from `https://www.cv.nrao.edu/~sransom/web/Ch6.html`).

a white dwarf spinning that fast couldn't hold together, and the timescale for pulsations (whether freefall, Eq. 198, or sound-crossing, Eq. 201) shouldn't be lower than a few seconds. And a black hole shouldn't have any surface with which to anchor coherent, precisely-repeatable EM radiation. Thus by process of elimination, a neutron star is the most likely culprit.

The phenomenological view is that an intense beam of EM radiation is misaligned with the neutron star's rotation axis. This presumably arises from a magnetic dipole misaligned with the NS's spin axis; nonetheless many details remain unclear, and pulsar emission mechanisms remain an active area of research. But it must somehow involve a rotating magnetic field generating a large electric field from equator to pole. This in turn accelerates electrons and generates synchrotron radiation that is highly coherent and highly polarized.

Rotation and Magnetic Fields

To explain the observed emission requires rapid rotation and an extremely strong magnetic field; both can be understood from basic conservation principles. As noted previously, white dwarfs typically have $P_{WD} \sim 1000$ s and $B \sim 10^6$ G (the Earth and Sun both have magnetic fields of just $\sim$1 G). Assuming angular momentum is conserved during the collapse from white dwarf to neutron star, then we should expect

$$I_{WD}\Omega_{WD} = I_{NS}\Omega_{NS} \tag{552}$$

and so

$$\frac{P_{NS}}{P_{WD}} = \frac{M_{NS}R_{NS}^2}{M_{WD}R_{WD}^2} \sim \left(10^{-3}\right)^2. \tag{553}$$

Thus we should expect

$$P_{NS} \sim 10^{-6}P_{WD} \sim 10^{-3} \text{ sec} \tag{554}$$

which is roughly consistent with the shortest periods seen in Fig. 48.

As for the strong magnetic field, that can also be inferred from the known field strengths of white dwarfs. Magnetohydrodynamics tells us that magnetic flux Φ_B is conserved through any surface moving with a plasma. Thus the magnetic flux through a loop enclosing solid angle $\Delta\Omega$ around either the WD progenitor or NS progeny should be

$$\Phi_B = B_{WD}\Delta\Omega R_{WD}^2 \approx B_{NS}\Delta\Omega R_{NS}^2 \tag{555}$$

and so

$$\frac{B_{NS}}{B_{WD}} \approx \left(\frac{R_{WD}}{R_{NS}}\right)^2 \approx 10^6. \tag{556}$$

Thus, we expect neutron stars to have surface magnetic field strengths of order 10^{12} G.

These strong magnetic fields induce an electromagnetic "backreaction,"

slowing the rotation over time. Unlike most stellar objects, which are in quasi-steady state, this spindown is precisely measured in many pulsars. The traditional value is the time derivative of the period, or $\dot{P}$ (i.e., P-dot), a dimensionless quantity plotted as the vertical axis of Fig. 48. Because neutron stars spin down we almost always see $\dot{P} > 0$ (i.e., spin period increasing). Occasionally some neutron stars will show transitory "glitches" indicating sudden rearrangements of their moments of inertia (like a spinning ice skater rearranging their limbs). Glitches are usually seen in young, relatively hot neutron stars whose interiors are still stabilizing and reaching a more stable equilibrium.

When P and $\dot{P}$ are plotted against each other as in Fig. 48, we obtain the observational equivalent of the HR diagram – but for neutron stars. The periods span a range of $10^{-3} - 10$ s, with a peak near 0.5 s; meanwhile $\dot{P}$ has a much broader range, from $10^{-20} - 10^{-10}$ with a peak near 10^{-15}. For the lowest values of $\dot{P}$, the emission from these pulsars is more stable than the most precise atomic clocks (which have comparable stabilities of $\sim 10^{-16}$).

Pulsar luminosity

Fig. 48 also lets us estimate the energy loss rate of pulsars. Assuming that their energy reservoir is mainly rotational kinetic energy, then (in the classical approximation)

(557)
$$E_{\rm rot} = \frac{1}{2} I \omega^2$$

(558)
$$= 2\pi^2 \frac{I}{P^2}$$

(559)
$$\approx \frac{4\pi^2}{5} M \left(\frac{R}{P}\right)^2$$

and so

(560)
$$\frac{dE}{dt} = \frac{d}{dt}\left(\frac{1}{2} I \omega^2\right)$$

(561)
$$= I \omega \dot{\omega}$$

(562)
$$= \frac{8\pi^2}{5} M \frac{R^2}{P^3} \dot{P}.$$

For the Crab Nebula ($P = 33$ ms, $\dot{P} \sim 10^{-13}$, $M_* \approx 1.5 M_\odot$, $R_* \approx 10$ km) we find

(563) $$L = -\frac{dE}{dt} \approx 10^{38} \text{ erg s}^{-1}$$

which is comparable to the bolometric luminosity of the entire Crab Nebula; pulsars essentially convert their rotational energy into light. (Also, note that this power far outstrips the Solar luminosity of $L_\odot \approx 4 \times 10^{33}$ erg s^{-1}).

The mechanism of that radiation, as previously noted, is the strong, rapidly rotating magnetic field. For a given magnetic moment m, the magnetic equivalent of the Larmor formula gives the emitted power as

$$P = \frac{2|\ddot{m}|^2}{3c^3}. \tag{564}$$

Following Rybicki & Lightman (pp. 323–324), the surface magnetic field is

$$B_0 = \frac{2m}{R^3}. \tag{565}$$

The component of $\vec{m}$ along the rotation axis is constant; given an angle α between the rotation and magnetic dipole axes,

$$|\ddot{\vec{m}}| = \omega^2 |\vec{m}| \sin\alpha. \tag{566}$$

Thus the total radiated power is

$$L = \frac{\sin^2\alpha}{6c^3} B_0^2 \omega^4 R^6. \tag{567}$$

Setting Eqs. 562 and 567 equal to each other, we see that

$$B_0^2 \propto P\dot{P} \tag{568}$$

and so the P-$\dot{P}$ diagram of Fig. 48 should allow us to directly estimate the magnetic field strength of a pulsar. Typical values are $10^8 - 10^{15}$ G; objects with the strongest fields are termed **magnetars**. These sometimes exhibit huge outbursts, affecting terrestrial satellites and modifying the Earth's ionosphere from kpc away.

Pulsar ages and the braking index

Most importantly, the combination of P and $\dot{P}$ allows us to estimate the age of a pulsar. If we assume that the spindown rate depends on the current spin rate to the n^{th} power, then

$$\dot{\omega} = a\omega^n. \tag{569}$$

If we fold in information about the second derivative,

$$\ddot{\omega} = an\omega^{n-1}\dot{\omega}, \tag{570}$$

then

$$\ddot{\omega}\omega = an\omega^n\dot{\omega}^2 \tag{571}$$

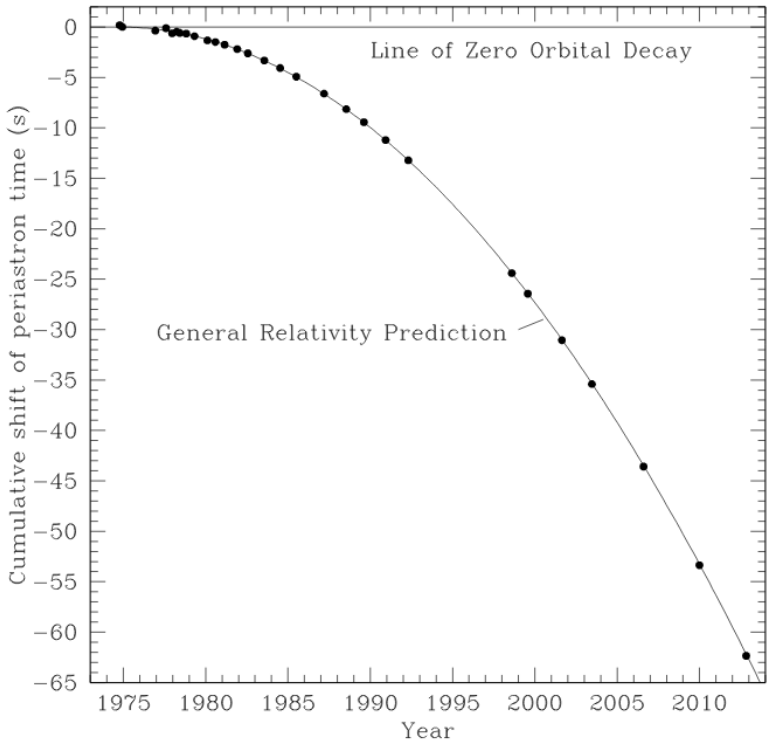

Figure 49: Period evolution of the famous Hulse-Taylor pulsar, with $P = 7.75$ hr.

and so

(572) $$n = \frac{\omega\ddot{\omega}}{\dot{\omega}^2}$$

is defined as the **braking index** of the pulsar. For magnetic dipole radiation as described by Eqs. 562 and 567, we have

(573) $$I\omega\dot{\omega} \propto \omega^4$$

and so the braking index $n = 3$ for pure magnetic dipole radiation.

Traditionally, one then models the period evolution as

(574) $$P(t) = ct^{1/(n-1)}$$

which yields

(575) $$\dot{P} = \frac{c}{n-1} t^{1/(n-1)-1} = \frac{P}{t(n-1)}$$

and so the **characteristic age** of a pulsar is given by

$$\tau_{\rm pulsar} = \frac{1}{n-1}\frac{P}{\ddot{P}} = \frac{P}{2\dot{P}} \quad (\text{for n} = 3). \tag{576}$$

Note from Eq. **??** that $\tau_{\rm pulsar}$ actually corresponds to the time for the period to increase by a factor of two. Nonetheless it's a pretty good age indicator: for the Crab pulsar ($P = 33$ ms, $\dot{P} = 4.2 \times 10^{-13}$) we find $\tau = 1200$ yr. Since this pulsar formed in SN 1054, our estimate is in pretty good agreement.

As seen for the Crab, characteristic ages are only approximate. Note from Fig. 48 that many millisecond pulsars have inferred ages > 10 Gyr, older than the universe! These are thought to have massively spun up by accreting high-angular-momentum material that inspiraled from a neighboring star (note that almost all ms pulsars are in binary systems). For other stars, the ages seem reasonable but the measured braking index (from P, $\dot{P}$, and $\ddot{P}$) is not 3.0 – for example, $n_{\rm crab} = 2.515 \pm 0.005$. This reflects the fact that the radiation is only approximately dipolar

Other tidbits, bibs, and bobs about pulsars:

- **Binary neutron stars.** When one (or both) of the objects in a binary is a neutron star, we can use the variations in the pulse arrival times to precisely map the orbit. Fig. 49 shows 40 years of data on the Hulse-Taylor pulsar, indicating inexorable inspiral of the binary due to emission of gravitational radiation. These provide excellent tests of GR, and also provide some of the most precise NS masses known.

- **Pulsar planets.** A diminutive, multibody of binary pulsars. It is not commonly known that the first confirmed planets beyond the Solar system were discovered by pulsar timing measurements. These revealed a three-planet system with orbital periods of 25, 66, and 98 days and masses of 0.02 (!!), 3.9, and 4.3 $M_\odot$, respectively. These have withstood the test of time, but they are not representative of the general population of extra-solar planets. Only ~ 6 such planets are known, in 3–4 systems.